

DOI: 10.1002/chem.201302630

Coumarinylmethyl Caging Groups with Redshifted Absorption

Ludovic Fournier,^[a] Isabelle Aujard,^[a] Thomas Le Saux,^[a, b] Sylvie Maurin,^[a]
Sandra Beaupierre,^[a] Jean-Bernard Baudin,^[a] and Ludovic Jullien*^[a, b]

Abstract: The small and synthetically easily accessible coumarinylmethyl backbone has been modified to generate a family of photolabile protecting groups with redshifted absorption. We relied on introducing electron-donating groups in the 7 position and electron-withdrawing groups in the 2-, and 2- and 3 positions. In particular, we

showed that the diethylamino-thiocoumarinylmethyl and the diethylamino-coumarinylidenemalononitrilemethyl are relevant for uncaging with cyan light.

Keywords: caged compounds • photochemistry • photolysis • protecting groups • UV/Vis spectroscopy

They both exhibit a significant action cross section for uncaging in the 470–500 nm wavelength range and a low light absorption between 350 and 400 nm. These attractive features are favorable to perform chromatic orthogonal photoactivation with UV and blue-cyan light sources, respectively.

Introduction

Photolabile protecting (caging) groups that can be cleaved after light absorption have recently proved attractive in various fields of Chemistry and Biology.^[1–13] In particular, caged molecules have been already used to study the dynamics of several biological processes with high spatio-temporal resolution.^[4–12] To be relevant in such experiments, the caging group must fulfill various requirements dealing with non-photophysical issues (access of the caged molecules to the biological targets, absence of any “dark” biological activity, etc.) but also depends on photophysics and on photochemistry (no biological effect of the illumination only, etc.). Hence, the large number of engineering constraints has led to the continuous introduction of new types of photolabile protecting groups. However, the most available caging groups still require ultraviolet (UV) light for photoactivation with one-photon excitation. This constraint may be significant to specifically analyze the effect of a photoreleased substrate at the level of the gene expression profile. Indeed, many endogenous biologically active molecules significantly absorb UV light, even in the Ultraviolet A range (UVA, 320–400 nm). Hence, illumination of riboflavin or flavin mononucleotide (FMN) can photosensitize triplet dioxygen^[14] and the resulting singlet state ¹O₂ can subsequently induce

mitogen-activated protein kinases (MAPK) such as p38 and c-Jun-N-terminal kinase (JNK).^[15,16] Carotenoids have been also incriminated since they are prone to UVA-induced photodegradation and are involved in the control of gene expression, either directly or through their ¹O₂ quenching action.^[17]

The first strategy to overcome the limit of a maximum of wavelength absorption lying below the 450 nm range requires the tailoring of new caging groups based on chromophores that absorb in the visible range. This approach has been implemented by Chen and Steinmetz, who adapted the rearrangement of an amino-substituted 1,4-benzoquinone to photorelease carboxylic acids and phenols upon illuminating at 542 nm.^[18,19] Wirz and Klan have explored the xanthene chromophore with absorption maxima in the 520 nm range.^[20] Ruthenium complexes have been used by Etchenique et al. to photorelease complexed amines upon illuminating in the 400–500 nm wavelength range.^[21–25] It is here also relevant to mention the intramolecular multichromophoric approach relying on an electron transfer from a photosensitizer molecule to a reducible protecting group, which is explored by Lee and Falvey,^[26] who showed it to be compatible with photoactivation in the visible range.^[27,28] The alternative strategy retains the established photochemistry with extension of the conjugation of the absorbing moiety. Depending on the investigated series, this approach has known successes^[29–31] but also limitations.^[32] Hence, we previously showed that the redshift absorption in the *ortho*-nitrobenzyl series was accompanied by a drop in the uncaging efficiency.^[32] In contrast, efficient caging groups with maxima up to 415 and to 450 nm, respectively, have been reported by Goldner et al. in the nitrophenethyl series^[29,30] and by Ellis-Davies et al. in the coumarinylmethyl series.^[31]

Among available photoremovable protecting groups, the coumarinylmethyl moiety has gained wide acceptance.^[31,33–36] It is compatible with caging multiple organic functions^[37–42]

[a] Dr. L. Fournier, Dr. I. Aujard, Dr. T. Le Saux, S. Maurin, S. Beaupierre, Prof. Dr. J.-B. Baudin, Prof. Dr. L. Jullien
Ecole Normale Supérieure, Département de Chimie
UMR CNRS-ENS-UPMC, Paris 06 8640 PASTEUR
24, rue Lhomond, 75231 Paris Cedex 05 (France)
E-mail: Ludovic.Jullien@ens.fr

[b] Dr. T. Le Saux, Prof. Dr. L. Jullien
UPMC Paris 06, 4, Place Jussieu
75232 Paris Cedex 05 (France)

Supporting information for this article is available on the WWW under <http://dx.doi.org/10.1002/chem.201302630>.

and exhibits large uncaging cross sections with two-photon excitation.^[37] Thus, many caged biologically-active compounds have been synthesized in this series.^[31, 34, 35, 37, 38, 40, 43, 44] Eventually, the mechanism leading to the photolytic release of the protected substrate has been extensively covered.^[45–47] In the context of caging groups, the coumarinylmethyl backbone has been already modified to shift its absorption spectrum up to the limit between the UV and visible ranges (≈ 450 nm), either by altering the substituents in the 3-^[31] or 7 position^[37, 38, 48–51] or after coumarin thionation.^[52, 53] However, literature data from various series of fluorophores have suggested that the coumarin platform could exhibit even more pronounced redshifted absorptions. In particular, up to the 600 nm range has been reached upon appropriately substituting the 2- and 3-coumarin positions.^[54, 55, 56]

In the present paper, we further explored the modification of the coumarin backbone to obtain new photolabile protecting groups with enhanced redshifted absorption. More specifically, we synthesized new coumarinylmethyl derivatives substituted in conjugated positions and studied their putative uncaging properties *in vitro*. The first section deals with the syntheses of two series of putative caged model compounds containing electron-donating groups in the 7 position and electron-withdrawing groups in the 2- and the 2- and 3 positions, respectively. The second section reports on the absorption and emission properties of the synthesized species. In the third section, we measure uncaging action cross sections for one-photon excitation. The final sections are devoted to the discussion and the concluding remarks.

Results

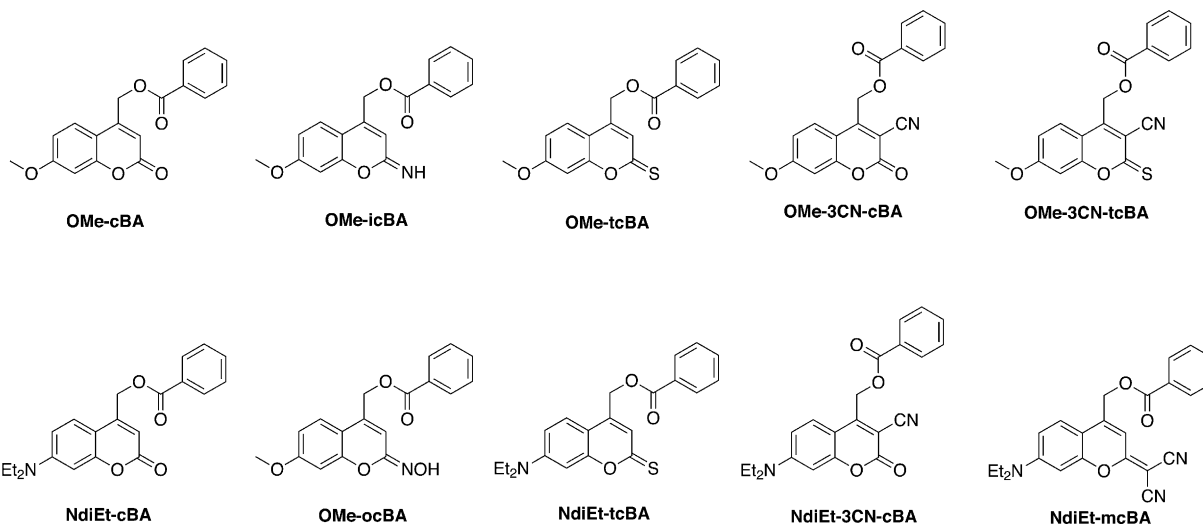
Design and syntheses

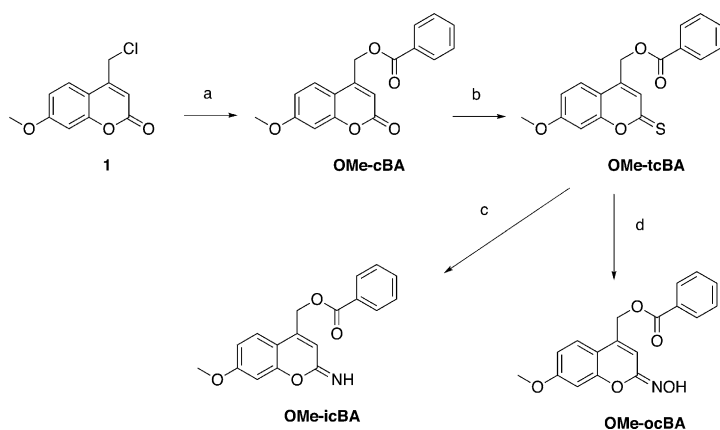
Design: In view of the literature results, we have first retained 1) the 4 position of the coumarin backbone to introduce the methylene for grafting the caged substrate and 2) an electron-donating group on the 7 position to cause

a redshift the absorption spectrum; we chose the methoxy and the diethylamino substituents. Moreover, to further redshift the light absorption, we considered increasing the photoinduced intramolecular charge-transfer by introducing electron-withdrawing groups on the 2- and 3 positions of the coumarin backbone. We first targeted replacement of the oxygen atom at the 2 position by various atoms and groups. Hence, we retained 1) the nitrogen atom, which becomes strongly electron-withdrawing when it is protonated and correspondingly gives rise to redshifted absorption;^[57] 2) the sulfur atom, in which 3d empty atomic orbitals can be involved in the intramolecular charge-transfer; 3) the conjugated vinylenic malonitrile motif, which is strongly electron-withdrawing. We also considered introducing an additional electron-withdrawing group at the 3 position. We have retained the cyano group, which can be introduced by various synthetic pathways and we did not expect this to significantly interfere with the coumarinylmethyl photochemistry except for a redshift in light absorption. The design of the putative caged model substrates was additionally governed by the nature of the groups to be protected. Since the coumarinylmethyl group is appropriate to cage acidic substrates (carboxylic acids, carbamic acids, etc.), we chose to cage a carboxylic acid with absorption properties that were not expected to alter the photochemical behavior of the coumarinylmethyl moiety: we adopted benzoic acid. Thus, we targeted the model compounds displayed below.

Their names of the caged benzoic acid model compounds originate from applying the following rules: 1) the prefixes **OMe** and **NdiEt** refer to the methoxy and diethylamino borne on the 7 position; 2) **3-CN** indicates the presence of a cyano group at the 3 position; 3) the letters **c** (O), **ic** (NH), **oc** (N(OH)), **tc** (S), and **mc** (C(CN)₂) precise the nature of the substituent at the 2 position; **BA** refers to benzoic acid

Syntheses: The syntheses of the 7-methoxy 3-non-substituted coumarins are displayed in Scheme 1. The **OMe-cBA** compound had been already obtained by esterification^[58] from

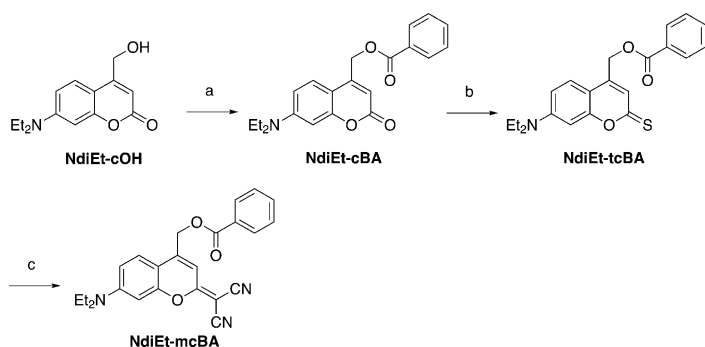




Scheme 1. Syntheses of the caged benzoic acid compounds in the 7-MeO-3-H series. a) Benzoic acid, KF, DMF, room temperature, 12 h, 71%; b) Lawesson's reagent, toluene, heated at reflux, 5 h, 78%; c) aq. NH_3 , EtOH, 60°C, 2 h, 3%; d) Hydroxylamine hydrochloride, sodium acetate, EtOH, RT, 3 h, 70%.

benzoic acid and 4-bromomethyl-7-methoxy-coumarin.^[59] Starting from 4-chloromethyl-7-methoxy-coumarin,^[60] we correspondingly used the same procedure to access **OMe-cBA** in 71% yield. Thiocoumarins (or coumarin thiones) can be obtained in good yields in one step from the corresponding coumarins by using Lawesson's reagent.^[61–64] Additional carboxylic esters are not affected under such conditions.^[62] We correspondingly converted **OMe-cBA** into **OMe-tcBA** by using Lawesson's reagent in toluene heated at reflux in 78% yield. Inspired by works in the thiocarbamide^[65] and thioester^[66] series, we used ammonia to transform **OMe-tcBA** into **OMe-icBA**. The resulting product decomposed on silica gel and it was purified by basic washing and extensive digestion with methanol to give the imino coumarin **OMe-icBA** with 3% yield. In contrast, the oximocoumarin **OMe-ocBA** was easily prepared in 70% yield from condensing hydroxylamine chlorhydrate in the presence of sodium acetate^[63,67] onto **OMe-tcBA**.

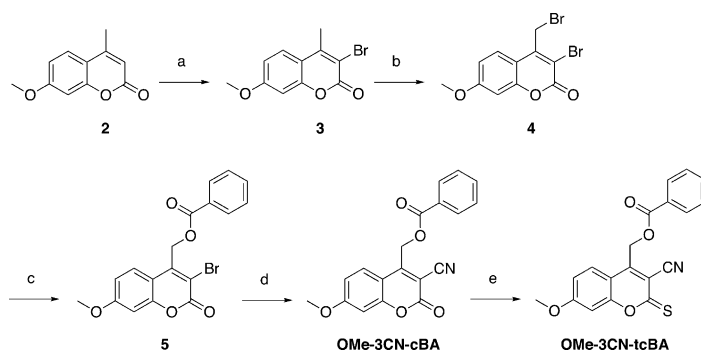
The syntheses of the 7-diethylamino 3-non-substituted coumarins are displayed in Scheme 2. Starting from the



Scheme 2. Syntheses of the caged benzoic acid compounds in the 7-NdiEt-3-H series. a) Benzoic acid, DCC, 4-dimethylaminopyridine (DMAP), CH_2Cl_2 , RT, 12 h, 75%; b) Lawesson's reagent, toluene, heat at reflux, 6 h, 84%; c) Malonitrile, PbO, Triethylamine, toluene, 90°C, 24 h, 56%.

commercially available 7-diethylamino-4-methylcoumarin, we first prepared the 7-diethylamino-4-hydroxymethylcoumarin **NdiEt-cOH** upon adapting the reported two-step procedures (SeO_2 , dioxane/water, heat at reflux, 14 days, 58%; NaBH_4 , ethanol, RT, 12 h, 72%).^[38,68] Compound **NdiEt-cOH** was then esterified with benzoic acid by using the coupling reagent *N,N*-dicyclohexylcarbodiimide (DCC) to yield the ester **NdiEt-cBA**^[69] in 75% yield. This ester was subsequently converted into the corresponding thiocoumarin **NdiEt-tcBA** (by using Lawesson's reagent, toluene, heat to reflux, 24 h) in 84% yield. In view of our poor results in the methoxy series, we did not attempt to synthesize the iminocoumarin **NdiEt-icBA**. In contrast, we prepared the dicyanocoumarin **NdiEt-mcBA** in 56% yield by condensing malonitrile onto the thiocoumarin **NdiEt-tcBA** in the presence of triethylamine^[70] and yellow lead oxide.^[71]

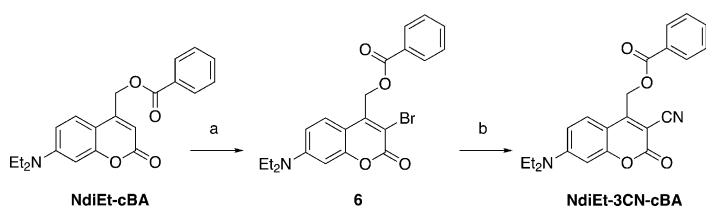
The syntheses of the 3-cyano-7-methoxy coumarins are displayed in Scheme 3. We aimed to introduce the cyano group in a coupling from the corresponding bromo deriva-



Scheme 3. Syntheses of the caged benzoic acid compounds in the 7-MeO-3-CN series. a) NBS, CHCl_3 , RT, 12 h, quantitative; b) NBS, CCl_4 , RT, 12 h, quantitative; c) Benzoic acid, KF, DMF, RT, 12 h, 90%; d) CuCN, NMP, 185°C, 1 h, 53%; e) Lawesson's reagent, toluene, heat at reflux, 5 h, 70%.

tive.^[72] Since we failed to directly introduce a bromine atom in the 3 position of **OMe-cBA**, we started from the 7-methoxy-4-methyl-coumarin **2**, which was selectively dibrominated at the 3 position and on the methyl group using a two-step procedure adapted from the literature to successively afford **3** and **4**.^[73] Benzoic acid was then esterified with the benzyl bromide **4** to give the benzoic ester **5** in 90% yield. The cyano group was eventually introduced in the 3 position by treatment of **5** with cuprous cyanide in *N*-methylpyrrolidone at 185°C to provide **OMe-3CN-cBA** in 53% yield. Compound **OMe-3CN-cBA** was further converted with the Lawesson's reagent in toluene into the corresponding thiocoumarin **OMe-3CN-tcBA** in 70% yield.

The syntheses of the 3-cyano-7-diethylamino coumarins are displayed in Scheme 4. In contrast to the 7-methoxy series, we adapted the experimental conditions (*N*-bromosuccinimide (NBS) in acetonitrile) to selectively introduce a bromine atom in the 3 position of the **NdiEt-cBA** coumarin and obtain **6** in 78% yield. Then, we substituted the

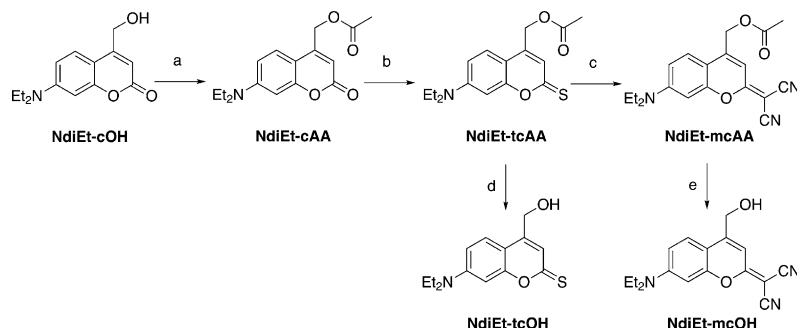


Scheme 4. Syntheses of the caged benzoic acid compounds in the 7-NdiEt-3-CN series. a) NBS, CH₃CN, RT, 2 h, 78%; b) CuCN, NMP, 180 °C, 1 h, 81%.

bromo for the cyano group by using CuCN in *N*-methyl-2-pyrrolidone (NMP) to give **NdiEt-3CN-cBA** in 81% yield.

In view of the promising results obtained during the preliminary uncaging experiments with **NdiEt-tcBA** and **NdiEt-mcBA** (see below), we eventually decided to synthesize the corresponding benzylic alcohols, **NdiEt-tcOH** and **NdiEt-mcOH**, to have reference compounds to analyze the forthcoming uncaging experiments, as well as to get starting materials appropriate to cage other substrates than benzoic acid.

We first considered relying on available synthons to access **NdiEt-tcOH** and **NdiEt-mcOH**. Thus, we attempted to treat **NdiEt-cOH** with the Lawesson's reagent in toluene but failed to obtain the desired thiocoumarin **NdiEt-tcOH**. We were also unable to cleanly hydrolyze the ester **NdiEt-tcBA** either under acidic or basic conditions. Therefore, we decided to synthesize a more labile ester than **NdiEt-tcBA**, which could react with malonitrile and be hydrolyzed to yield both **NdiEt-tcOH** and **NdiEt-mcOH** (Scheme 5). Thus, the alcohol **NdiEt-cOH** was esterified with acetic acid by using DCC to provide the ester **NdiEt-cAA** in 85% yield. This ester was subsequently transformed into the corresponding thiocoumarin **NdiEt-tcAA** (Lawesson's reagent, toluene, heated at reflux, 6 h) in 92% yield. The latter thiocoumarin was subsequently hydrolyzed (1.25 M HCl in ethanol, heated at reflux, 15 h) to provide the first targeted alcohol **NdiEt-tcOH** in 75% yield. **NdiEt-tcAA** was also treated with malonitrile in the presence of 4-dimethylaminopyridine and yellow lead oxide to afford the ester **NdiEt-mcAA** with 85% yield. The second targeted alcohol **NdiEt-mcOH** was eventually obtained in 97% yield upon hydrolyzing **NdiEt-mcAA** under acidic conditions.



Scheme 5. Syntheses of the caging alcohols in the 7-NdiEt-3-H series. a) Acetic acid, DCC, DMAP, CH₂Cl₂, RT, 12 h, 85%; b) Lawesson's reagent, toluene, heat at reflux, 6 h, 92%; c) Malonitrile, PbO, DMAP, toluene, 90 °C, 24 h, 85%; d) and e) 1.25 M HCl in ethanol, heat at reflux, 15 h, 75 and 97%, respectively.

Absorption and emission properties: In view of possible biological applications, the following in vitro physicochemical experiments were performed in a mixture of water and an organic solvent (for substrate dissolution). We adopted 20 mM Tris pH 7.5/acetonitrile (1:1, v/v).

In a first step, we analyzed the absorption properties of the putative caged model compounds and of the corresponding alcohols. We also examined the luminescence emission of the investigated compounds, which may be significant for biological applications. Indeed, it may be essential to avoid any interference between the emission from the starting caged molecule and from the released substrate (tracer applications) or from any species produced after substrate release (detection of a biological response to a stimulus). The main features of the absorption and emission properties of the putative caged model compounds and the corresponding alcohols are given in Table 1.

The absorption maxima are within the 320–430 and 380–490 nm wavelength ranges in the 7-methoxy and 7-diethylamino series, respectively, with molar absorption coefficients between 7000 and 35000 M⁻¹ cm⁻¹. The molar absorption coefficients of the most redshifted species (**NdiEt-3CN-cBA**, **NdiEt-tcBA**, and **NdiEt-mcBA**) are also interestingly ten times lower around 365 nm than at their maximal absorption wavelength.

Our results satisfactorily compare with the absorption properties of similar chromophores. For instance, **OMe-cBA** was reported to exhibit $\lambda_{\text{max}} = 324$ nm and $\epsilon = 13000$ M⁻¹ cm⁻¹ in a similar solvent.^[46] Moreover, the absorption maxima and molar absorption coefficients of 7-diethylamino-4-methyl-thiocoumarin ($\lambda_{\text{max}} = 460$ nm and $\epsilon = 28900$ M⁻¹ cm⁻¹) and 7-diethylamino-4-methyl-coumarylidene malononitrile ($\lambda_{\text{max}} = 475$ nm and $\epsilon = 31600$ M⁻¹ cm⁻¹) reported in ethanol^[55] are in agreement with the results of **NdiEt-tcOH** and **NdiEt-mcOH**.

All other things being equal, the absorption maxima in the diethylamino series are redshifted with respect to the methoxy one. This observation was anticipated from the lower electronegativity of the nitrogen atom leading to a larger charge-transfer in the excited state. One can similarly observe that the absorption maximum shifts to larger values when the withdrawing electronic-demand of the atom/group in the 2- (compare O, NH, NH₂⁺, S, C(CN)₂) and 3 positions (compare -H and -CN) of the coumarin backbone is increased. Eventually, one notices that the benzoic esters **NdiEt-tcBA** and **NdiEt-mcBA** exhibit larger values of their absorption maximum and molar absorption coefficient than their benzyl alcohol counterparts **NdiEt-tcOH** and **NdiEt-mcOH**.

Similar trends were observed with the emissive properties (see Table 1). Our observations

Table 1. Absorption and emission properties of the putative caged model compounds and of the corresponding alcohols.^[a]

Compound	$\lambda_{\text{max}}^{(1)}$ [nm]	$\epsilon(\lambda_{\text{max}}^{(1)})$, $\epsilon(365)$ [$\text{mM}^{-1}\text{cm}^{-1}$]	$\lambda_{\text{em}}^{(1)}$ [nm], $(\Phi_{\text{L}}^{(1)})$ [%]
OMe-cBA	323	13.5, 0.4	396, (14)
OMe-icBA (pH 8.5) ^[b]	325	7, 3	–
OMe-icBA (pH 5.0) ^[b]	330	6.5, 5	–
OMe-ocBA	330	14, 3.5	394, (1)
OMe-tcBA	398	17, 10	– ^[c]
OMe-3CN-cBA	360	20.5, 20	422, (64)
OMe-3CN-tcBA	427	18.5, 5	– ^[c]
NdiEt-cBA	385	24, 17.5	493, (11)
NdiEt-cOH	379	17, 14.5	478, (18)
NdiEt-3CN-cBA	443	26, 2	503, (1)
NdiEt-tcBA	472	31, 2.5	578, (2)
NdiEt-tcOH	467	23.5, 1	551, (1)
NdiEt-mcBA	487	33, 3.5	561, (17)
NdiEt-mcOH	478	32.5, 3	552, (19)

[a] Maxima of single-photon absorption $\lambda_{\text{max}}^{(1)}$, and of steady-state luminescence emission after one-photon excitation $\lambda_{\text{em}}^{(1)}$, molar absorption coefficients for single-photon absorption at $\lambda^{(1)}$, $\epsilon(\lambda^{(1)})$ ($\pm 5\%$), quantum yields of luminescence after one-photon excitation $\Phi_{\text{L}}^{(1)}$ ($\pm 10\%$). Solvent: acetonitrile/Tris pH 7.5 buffer (20 mM) 1:1 (v/v) except for **OMe-icBA**. [b] The pH was fixed at 8.5 in the 20 mM Tris buffer for the pH 8.5 experiment, whereas we used a 20 mM pH 5.0 acetate buffer instead of the Tris buffer for the pH 5.0 experiment. A pK in the 7.5 range has been reported for iminocoumarins.^[57] [c] Too weakly luminescent to extract reliable values.

are in line with literature results when taking into account solvatochromic effects. Hence, the emission wavelength of **NdiEt-cBA** satisfactorily compares to the one of a reported phosphoric ester in a similar solvent.^[38] In contrast, the emission wavelengths observed for **NdiEt-tcOH** and **NdiEt-mcOH** are significantly redshifted with respect to the reported values for 7-diethylamino-4-methyl-thiocoumarin ($\lambda_{\text{max}} = 515$ nm) and 7-diethylamino-4-methyl-coumarylidene-malononitrile ($\lambda_{\text{max}} = 522$ nm) in ethanol.^[55] In fact, this discrepancy originates from the positive solvatochromism of the thiocoumarin and of the coumarylidene-malononitrile (see the Supporting Information): we recorded consistent values in ethanol.

Substituent effects are close to the ones observed in absorption and for the same reasons: All other things being equal, emission is more redshifted 1) in the diethylamino series than in the methoxy one, 2) when the withdrawing effect of the atom/group in the 2- and 3 positions of the coumarin backbone is increased, 3) in the benzoic esters **NdiEt-tcBA** and **NdiEt-mcBA** than in the corresponding benzyl alcohols **NdiEt-tcOH** and **NdiEt-mcOH**.

Eventually, the observed quantum yields of luminescence cover a large range (from vanishing to large values) and they exhibit contrasting trends. In the coumarin series, which is the most fluorescent, we observed that the methoxy series is more emissive than the diethylamino series (compare **OMe-cBA** and **NdiEt-cBA**, and **OMe-3CN-cBA** and **NdiEt-3CN-cBA**). This behavior is in agreement with previous observations.^[45] We observed an opposite trend in the thiocoumarin series (compare **OMe-tcBA** and **NdiEt-tcBA**), which is overall poorly emissive as already observed by

Tkach.^[55] This different behavior may originate from the nature of luminescence in the thiocoumarin series. Indeed, phosphorescence instead of fluorescence has been invoked to account for emission of thiones.^[74–76]

Preliminary screening of the photochemical properties: In a first step we screened the putative caged model compounds for their thermal stability as well as for their photolysis after one-photon absorption upon illuminating at a common absorption wavelength (365 nm), which is representative of the absorption range of most present caging groups.

To evaluate the thermal stability, we recorded the temporal evolution of the absorption spectrum of 25 μM solutions in 20 mM pH 7.5 Tris buffer/acetonitrile 1:1 (v/v) in the dark at room temperature. Two compounds (**OMe-icBA** and **OMe-3CN-tcBA**) exhibited an absorbance change at the 3 h timescale; those compounds were discarded for the subsequent experiments. In contrast, the eight remaining model compounds proved stable at the 3 h timescale and their photochemical features were examined.^[77]

We submitted the remaining 25 μM solutions in 20 mM pH 7.5 Tris buffer/acetonitrile (v/v) to the illumination of a benchtop UV lamp mostly emitting at 365 nm. In this series of experiments, we mainly focused on evidencing any uncaging process leading to the photorelease of benzoic acid. Aliquots were extracted after increasing illumination durations. We analyzed the temporal dependence of the absorption spectrum and of the concentration in benzoic acid measured by HPLC (see Figure 11S, the Supporting Information). Except in the case of **OMe-ocBA**,^[78] UV illumination altered the absorption spectrum and simultaneously led to the photorelease of benzoic acid. Figure 1 displays the typical results (see also Figures 12S–16S, the Supporting Information). In the investigated range of illumination durations, two different behaviors have been encountered. Figure 1 a and b display the behavior associated to a “fast” photoinduced release of benzoic acid. The curvature observed in the temporal dependence of both the normalized absorbance and of the concentration in photoreleased benzoic acid enabled the extraction of the action uncaging cross section, the uncaging quantum yield, the molar absorption coefficient of the photoproducts, and the final concentration in photoreleased benzoic acid (see the Experimental Section). In contrast, Figure 1 c and d show the behavior corresponding to the regime of “slow” photoinduced release of the caged substrate. The observed temporal dependences are now linear. Since we did not investigate the nature of the photoproducts at that step, their photophysical properties have remained unknown so as to restrict the extraction of the photochemical parameters associated to uncaging from the temporal dependence of the concentration in photoreleased benzoic acid (see the Experimental Section). The overall results are given in Table 2.

In view of the wide acceptance of the diethylamino coumarinylmethyl moiety as a caging group, we used the results obtained with **NdiEt-cBA** to define a threshold to further

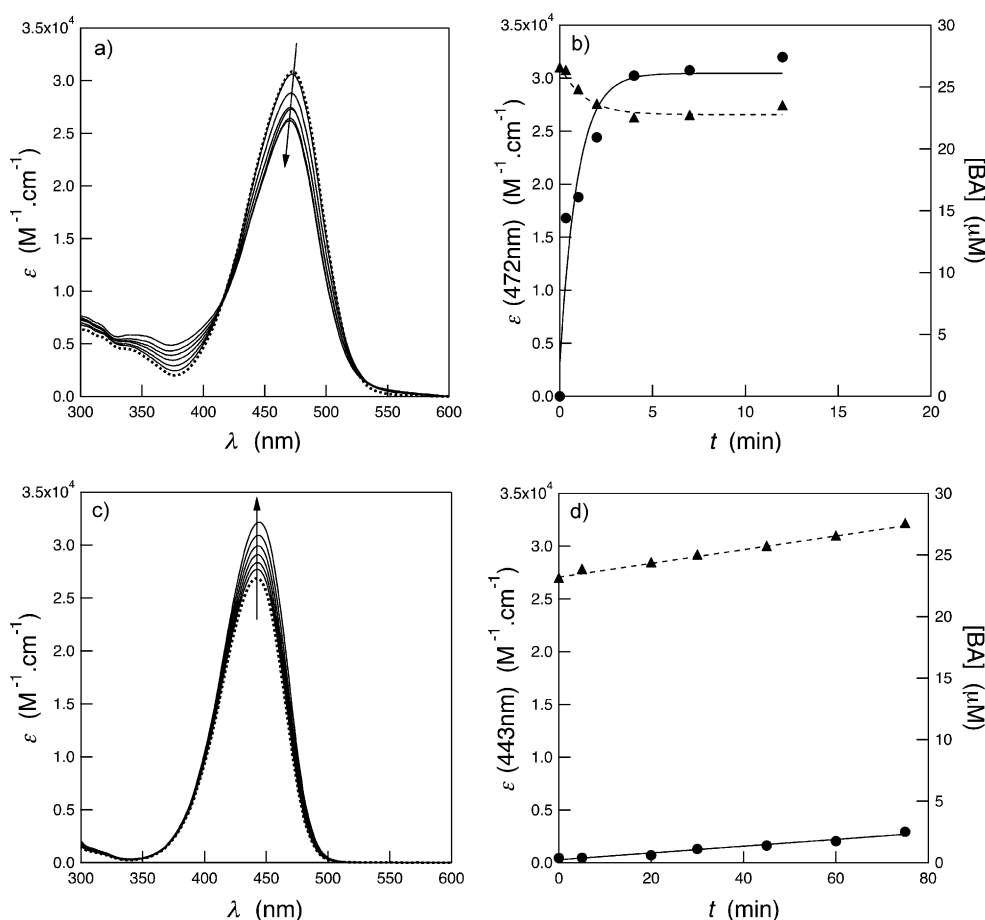


Figure 1. Evolution of solutions (25 μM) of two caged-model compounds (**NdiEt-tcBA** in a and b, and **NdiEt-3CN-cBA** in c and d) upon illuminating at 365 nm for various durations ($I_0(365) = 5.8 \times 10^{-5} \text{ Ein min}^{-1}$; $t(\text{min}) = 0, 0.3, 1, 2, 4, 7, \text{ and } 12$ in a and b, and 0, 5, 20, 30, 45, 60, 75 in c and d. a and c) Temporal evolution of the solution absorbance divided by its concentration to afford its molar absorption coefficient $\epsilon(\lambda^{(1)})$ (the initial absorption spectrum is drawn with a dotted line); b and d) Temporal dependence of the normalized absorption coefficient at the absorption maximum $\epsilon(\lambda_{\text{max}}^{(1)})$ (▲). The associated exponential (with Eq. (9), see the Supporting Information, in b) or linear (with Eq. (10), see the Supporting Information, in d) fit is shown as a dotted line. For **NdiEt-tcBA**, we extracted $k_u^{(1)} = (0.8 \pm 0.3) \text{ min}^{-1}$ and $\epsilon(472, \infty) = (27000 \pm 1000) \text{ M}^{-1} \text{ s}^{-1}$ from the exponential fit; b and d) Temporal evolution of the concentration [BA] of benzoic acid extracted from the HPLC chromatogram (●). The exponential (with Eq. (6), see the Supporting Information, in b) or linear (with Eq. (7), see the Supporting Information, in d) fit is shown as a solid line. For **NdiEt-tcBA** and **NdiEt-3CN-cBA**, we respectively extracted $k_u^{(1)} = (1.0 \pm 0.4) \text{ min}^{-1}$ and $[\text{BA}]_{\infty} = (26 \pm 6) \mu\text{M}$, and $k_u^{(1)} = (0.001 \pm 0.0004) \text{ min}^{-1}$ using 25 μM for the initial concentration in caged compound. Solvent: 20 mM pH 7.5 Tris buffer/acetonitrile (v/v). $T = 293 \text{ K}$.

screen the uncaging properties. In fact, our present $1\text{--}3 \times 10^{-3}$ range for $\Phi_u^{(1)}(365)$ fairly compares with results reported for a similar caged group (a carbonate) in a related solvent mixture (potassium 3-(*N*-morpholino)propanesulfonic acid (KMOPS), pH 7.2 buffer/acetonitrile, 3:1 v/v).^[40] Hence, three caged-model compounds (**OMe-cBA**, **OMe-tcBA**, and **OMe-3CN-cBA**) were estimated to exhibit too poor photochemical properties and were not further examined. In contrast, we eventually retained three caged-model compounds (**NdiEt-3CN-cBA**, **NdiEt-tcBA**, and **NdiEt-mcBA**), which were shown to quantitatively photorelease benzoic acid at rates similar or larger than the ones of **NdiEt-cBA**. They were subsequently examined in more detail upon illuminating at their absorption maximum.

In a first step we relied on the reference **NdiEt-cBA** to set up our spectrometric protocol for analyzing the uncaging process. We submitted a solution of **NdiEt-cBA** (5 μM) in

20 mM pH 7.5 Tris buffer/acetonitrile (v/v) to the illumination of the 75 W xenon lamp of a spectrofluorometer at 385 nm and we recorded the absorption spectrum of the solution after various illumination times. Upon increasing the illumination duration, Figure 17S a (the Supporting Information) shows that the absorbance 1) blueshifts from 385 to 378 nm and 2) drops (the molar absorption coefficient at 385 nm decreases from 24000 to 17000 $\text{M}^{-1} \text{ cm}^{-1}$). Since the photoreleased benzoate anion did not contribute to the absorbance in the investigated wavelength range, it was noticeable that the absorbance of the illuminated **NdiEt-cBA** solution asymptotically tends to the absorbance of the reference alcohol **NdiEt-cOH** (see Table 1). From the exponential decay of the normalized absorbance on time (Figure 17S b, the Supporting Information), we derived the **NdiEt-cBA** photo-consumption rate constant $k_u^{(1)} = (0.065 \pm 0.002) \text{ min}^{-1}$. After calibration of the photon flux at the sample, we ex-

Table 2. Action uncaging cross section of the caged model compounds for one-photon excitation at $\lambda_{\text{exc}}^{(1)} = 365$ nm, $\varepsilon(365)\Phi_u^{(1)}(365)$ (in $\text{M}^{-1}\text{cm}^{-1}$), and quantum yield of uncaging after one-photon excitation $\Phi_u^{(1)}(365)$, as measured from the temporal dependence of the normalized absorbance or of the concentration in photoreleased benzoic acid measured by HPLC.^[a]

Compound	Thermal stability ^[b]	$\varepsilon_u(365)\Phi_u^{(1)}(365)$ [$\text{M}^{-1}\text{cm}^{-1}$]	$10^2\Phi_u^{(1)}(365)$	$\varepsilon(\lambda_{\text{max}}^{(1)\infty})$ ^[c] [$\text{mm}^{-1}\text{cm}^{-1}$]	$\varepsilon_u(365)\Phi_u^{(1)}(365)$ [$\text{M}^{-1}\text{cm}^{-1}$]	$10^2\Phi_u^{(1)}(365)$	$[\text{BA}]_{\infty}$ ^[d] [μM]
OMe-cBA	Yes	–	–	–	0.16 ± 0.04	0.04 ± 0.01	–
OMe-icBA (pH 8.5)	No	–	–	–	–	–	–
OMe-icBA (pH 5.0)	No	–	–	–	–	–	–
OMe-ocBA	Yes	–	–	–	–	–	–
OMe-tcBA	Yes	–	–	–	0.4 ± 0.2	0.002 ± 0.001	–
OMe-3CN-cBA	Yes	–	–	–	1.0 ± 0.2	0.005 ± 0.001	–
OMe-3CN-tcBA	No	–	–	–	–	–	–
NdiEt-cBA	Yes	52 ± 35	0.3 ± 0.2	19 ± 1	17 ± 2	0.1 ± 0.01	29 ± 2
NdiEt-3CN-cBA	Yes	–	–	–	0.9 ± 0.2	0.05 ± 0.01	–
NdiEt-tcBA	Yes	240 ± 80	9 ± 3	27 ± 1	320 ± 130	12 ± 5	23 ± 6
NdiEt-mcBA	Yes	4.3 ± 2.3	0.13 ± 0.08	0 ± 2	2.3 ± 1.3	0.07 ± 0.04	16 ± 8

[a] When an exponential fit was used to analyze the data, the asymptotic normalized absorbance at the absorption maximum, $\varepsilon(\lambda_{\text{max}}^{(1)\infty})$, or concentration in benzoic acid, $[\text{BA}]_{\infty}$, is given in the Table. Initial concentration in caged model compound: $25 \mu\text{M}$; Solvent: acetonitrile/Tris pH 7.5 buffer (20 mM). See the main text and the Experimental Section. [b] Yes/No indicates whether any significant change of the absorption spectrum was observed at the 3 h timescale. [c] Measured from the temporal dependence of the normalized absorbance. [d] Measured from the temporal dependence of the concentration in photoreleased benzoic acid measured by HPLC.

tracted from the rate constant $\Phi_u^{(1)} = (2.1 \pm 0.2) \times 10^{-3}$ and $\varepsilon_u(385)\Phi_u^{(1)} = (51 \pm 5) \text{M}^{-1}\text{cm}^{-1}$, respectively, for the quantum yield of uncaging and for the uncaging action cross section with one-photon excitation at $\lambda_{\text{max}}^{(1)} = 385$ nm. These results were in fair agreement with our observations at 365 nm (see Table 2). Therefore, we considered that this experiment validated our protocol for measuring action uncaging cross sections and uncaging quantum yields. Thus, we submitted solutions of **NdiEt-3CN-cBA**, **NdiEt-tcBA**, and **NdiEt-mcBA** in 20 mM pH 7.5 Tris buffer/acetonitrile (v/v) to the illumination of the 75 W xenon lamp of a spectrofluorometer at 443, 472, and 487 nm, respectively, and analyzed the temporal dependence of their absorption spectrum. Furthermore adopting a concentration of $25 \mu\text{M}$ allowed us to measure the concentration in photoreleased benzoic acid by using HPLC. The results are displayed in Figures 2–4.

Upon increasing the illumination duration, Figure 2a shows that the absorbance of the **NdiEt-3CN-cBA** solution 1) blueshifts from 443 to 430 nm and 2) drops (the molar absorption coefficient at 443 nm decreases from $25\,900$ to $16\,500 \text{M}^{-1}\text{cm}^{-1}$). The normalized absorbance exponentially decays with time (Figure 2b) with an associated rate constant equal to $(0.015 \pm 0.003) \text{min}^{-1}$ and $15\,000 \text{M}^{-1}\text{cm}^{-1}$ for the asymptotic value of the molar absorption coefficient of the solution. In the meantime, the concentration in benzoic acid exponentially increases with a rate constant of $(0.014 \pm 0.002) \text{min}^{-1}$ and converges towards $15 \mu\text{M}$. The latter result evidenced that the uncaging of **NdiEt-3CN-cBA** occurred in one step at the considered timescale in good yield. After

calibration of the photon flux at the sample, we extracted from the average **NdiEt-3CN-cBA** photo-consumption rate constant $k_u^{(1)}: \Phi_u^{(1)} = (4 \pm 1) \times 10^{-4}$ and $\varepsilon_u^{(1)}(443)\Phi_u^{(1)} = (9 \pm 2) \text{M}^{-1}\text{cm}^{-1}$, respectively, for the quantum yield of uncaging and for the uncaging action cross section with one-photon excitation at $\lambda_{\text{max}}^{(1)} = 443$ nm (see Table 3).

Figure 3a shows that the temporal evolution of the absorbance of the **NdiEt-tcBA** solution was more complex. In a first kinetic regime, the absorbance slightly blueshifts from 472 to 467 nm and drops from $\varepsilon(472, \infty) = (30\,000 \pm 1\,000) \text{M}^{-1}\text{cm}^{-1}$ to $\varepsilon(467, \infty) = (25\,000 \pm 1\,000) \text{M}^{-1}\text{cm}^{-1}$, yielding an absorption spectrum that interestingly compared with the one of the **NdiEt-tcOH** alcohol. Then, we observed the gradual disappearance of the absorption band at 467 nm simultaneously occurring with an absorption

band growth at 365 nm. As displayed in Figure 3b, such a behavior could be satisfactorily fitted to a biexponential associated to rate constants of $(9 \pm 1) \text{min}^{-1}$ and $(0.016 \pm 0.001) \text{min}^{-1}$ with a vanishing asymptotic value of the molar absorption coefficient of the solution. In the meantime, the concentration in benzoic acid exponentially increases with a rate constant of $(9 \pm 1) \text{min}^{-1}$ and converges towards $22 \mu\text{M}$ (Figure 3c). The similarity between the largest rate constants observed by UV absorption and HPLC suggested that the first kinetic regime was associated with the quantitative uncaging of **NdiEt-tcBA**. After calibration of the photon flux at the sample, from **NdiEt-tcBA** we extracted the photo-consumption rate constant $k_u^{(1)}: \Phi_u^{(1)} = (18 \pm 2) \times 10^{-2}$ and $\varepsilon_u^{(1)}(472)\Phi_u^{(1)} = (5\,600 \pm 600) \text{M}^{-1}\text{cm}^{-1}$ for the quantum yield of uncaging and for the uncaging action cross section with one-photon excitation at $\lambda_{\text{max}}^{(1)} = 472$ nm (see Table 3).

In view of the existence of the second kinetic regime, the photoconversion of the **NdiEt-tcBA** solution was further investigated by analyzing the temporal evolution of the concentrations of the **NdiEt-tcBA** reactant and of the putative photoproducts by using HPLC (Figure 3d). The decay rate of $(9 \pm 3) \text{min}^{-1}$ associated with the total **NdiEt-tcBA** photo-conversion was in line with the preceding uncaging interpretation. Moreover, HPLC confirmed that **NdiEt-tcOH** alcohol formation at $(7 \pm 2) \text{min}^{-1}$ quantitatively resulted from **NdiEt-tcBA** photoconversion. Furthermore, **NdiEt-tcOH** was suggested to exponentially degrade at longer times with a rate constant of $(0.008 \pm 0.007) \text{min}^{-1}$, which corresponded to $\Phi_d^{(1)} = (2.5 \pm 0.5) \times 10^{-4}$ and $\varepsilon_d^{(1)}(\lambda_{\text{max}}^{(1)})(472)\Phi_d^{(1)} = (5.6 \pm$

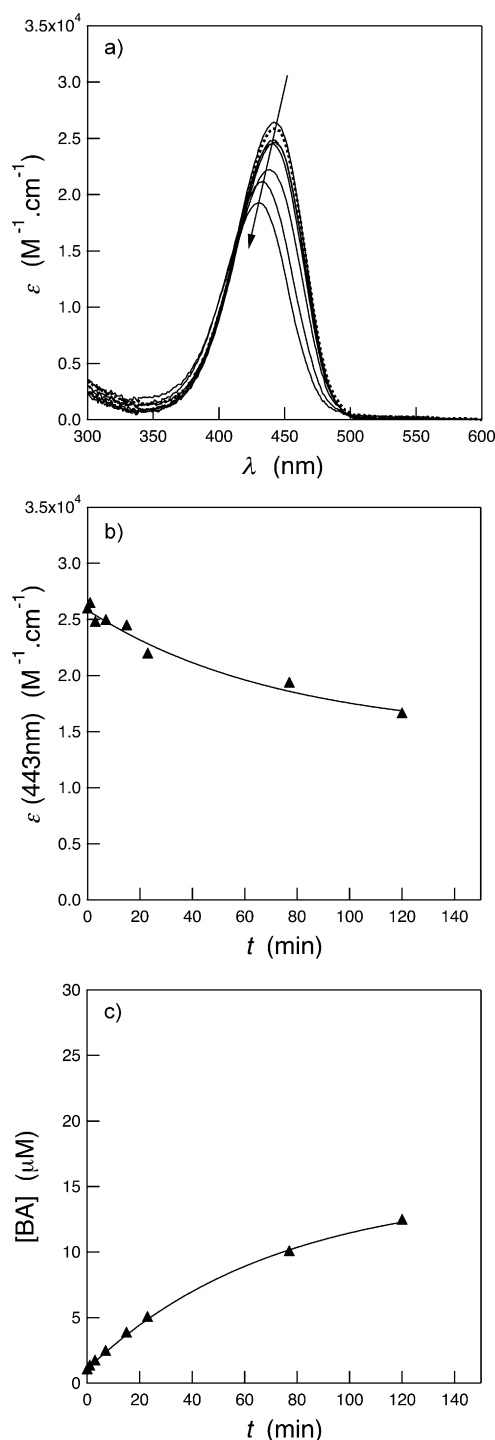


Figure 2. Evolution of a solution of **NdiEt-3CN-cBA** ($25 \mu\text{M}$) upon illuminating at 443 nm for various durations $t(I_{0,443}) = 3.15 \times 10^{-6} \text{ Ein min}^{-1}$; $t(\text{min}) = 0, 1, 3, 7, 15, 23, 77, \text{ and } 120$). a) Temporal evolution of the solution absorbance divided by its concentration to afford its molar absorption coefficient $\epsilon(\lambda^{(1)})$ (the initial absorption spectrum is drawn with a dotted line); b) Temporal dependence of the normalized absorption coefficient at the absorption maximum $\epsilon(443)$ (▲). The associated exponential fit with Eq. (9) (see the Supporting Information) is shown as a solid line. We extracted $k_u^{(1)} = (0.015 \pm 0.002) \text{ min}^{-1}$ and $\epsilon(443, \infty) = (15000 \pm 1000) \text{ M}^{-1} \text{ cm}^{-1}$ from the exponential fit; c) Temporal evolution of the concentration $[\text{BA}]$ of benzoic acid extracted from the HPLC chromatogram (▲). The exponential fit with Eq. (6) (see the Supporting Information) shown as a solid line yields $k_u^{(1)} = (0.014 \pm 0.002) \text{ min}^{-1}$ and $[\text{BA}]_{\infty} = (15 \pm 3) \mu\text{M}$. Solvent: $20 \text{ mM pH } 7.5 \text{ Tris buffer/acetonitrile (v/v)}$. $T = 293 \text{ K}$.

$1.1) \text{ M}^{-1} \text{ cm}^{-1}$ for the quantum yield of degradation and for the degradation action cross section with one-photon excitation at $\lambda_{\text{max}}^{(1)} = 472 \text{ nm}$ (see Table 4). This observation was confirmed by an independent **NdiEt-tcOH** illumination experiment (Figure 21S, the Supporting Information), which similarly provided $\Phi_d^{(1)} = (2.3 \pm 0.1) \times 10^{-4}$ for the quantum yield of degradation with one-photon excitation at $\lambda_{\text{max}}^{(1)} = 472 \text{ nm}$.^[79]

The degradation rate constant observed by HPLC fairly compared with the second rate constant observed by UV/Vis absorption. This agreement led us to assume that the thiocoumarine chromophore disappeared during the degradation step. Hence, upon considering the rise of an absorption band in the range expected for the coumarin chromophore, we examined whether the formation of **NdiEt-cOH** occurred during **NdiEt-tcOH** degradation. Indeed, we observed the exponential growth of a peak associated with the formation of a photoproduct exhibiting the molecular weight of **NdiEt-cOH** with a rate constant of $(0.018 \pm 0.003) \text{ min}^{-1}$, in line with the degradation rate. By using a sample of **NdiEt-cOH** for calibration, our analysis suggested that the photoconversion of **NdiEt-tcOH** into **NdiEt-cOH** was not quantitative (typically in the 35% yield) making the formation of other photoproducts likely.

Figure 4a displays the temporal evolution of the absorbance of the **NdiEt-mcBA** solution. We observed that the absorbance slightly blueshifts from 487 to 482 nm and drops from $\epsilon(487, \infty) = (33000 \pm 1000) \text{ M}^{-1} \text{ cm}^{-1}$ to $\epsilon(482, \infty) = (17500 \pm 1000) \text{ M}^{-1} \text{ cm}^{-1}$. Whereas the range of absorption wavelength is in the range expected for the **NdiEt-mcOH** alcohol (see Table 1), the asymptotic molar absorption coefficient would be notably low for the diethylamino-coumarylidene malononitrile chromophore. As displayed in Figure 4b, the absorbance drop could be satisfactorily fitted to a mono-exponential associated to a rate constant of $(0.018 \pm 0.001) \text{ min}^{-1}$ with the asymptotic value of the molar absorption coefficient of the solution being $\epsilon(487, \infty) = (17000 \pm 1000) \text{ M}^{-1} \text{ cm}^{-1}$. In the meantime, the concentration in benzoic acid exponentially increases with a rate constant of $(0.016 \pm 0.001) \text{ min}^{-1}$ and converges towards $26 \mu\text{M}$, which suggested that the uncaging was quantitative. After calibration of the photon flux at the sample, we extracted from the **NdiEt-mcBA** photo-consumption rate constant $k_u^{(1)}$: $\Phi_u^{(1)} = (3.4 \pm 0.4) \times 10^{-4}$ and $\epsilon_u^{(1)}(487) \Phi_u^{(1)} = (11 \pm 1) \text{ M}^{-1} \text{ cm}^{-1}$ for the quantum yield of uncaging and for the uncaging action cross section with one-photon excitation at $\lambda_{\text{max}}^{(1)} = 487 \text{ nm}$ (see Table 3).

Beyond the desired observation of **NdiEt-mcBA** uncaging liberating benzoic acid, the unexpected absorbance behavior motivated us to further analyze the nature of the co-product resulting from **NdiEt-mcBA** illumination. In analogy to **NdiEt-tcOH**, we first hypothesized that the **NdiEt-mcOH** alcohol could be formed in a first step and then reacts photochemically. After checking for the thermal stability of **NdiEt-mcOH**, we correspondingly exposed a solution of **NdiEt-mcOH** ($25 \mu\text{M}$) at 487 nm under the illumination conditions, which had been used with **NdiEt-mcBA** (see Fig-

Table 3. Action uncaging cross section of the caged model compounds **NdiEt-cBA**, **NdiEt-3CN-cBA**, **NdiEt-tcBA**, and **NdiEt-mcBA** for one-photon excitation at $\lambda_{\max}^{(1)}$, $\epsilon_u(\lambda_{\max}^{(1)})\Phi_u^{(1)}(\lambda_{\max}^{(1)})$ (in $\text{M}^{-1}\text{cm}^{-1}$) and the quantum yield of uncaging after one-photon excitation $\Phi_u^{(1)}(\lambda_{\max}^{(1)})$, as extracted from the temporal dependence of the normalized absorbance and the concentration in photoreleased benzoic acid as measured by HPLC.^[a]

Compound	[cBA] ₀ [μM]	$\lambda_{\max}^{(1)}$ [nm]	$\epsilon_u(\lambda_{\max}^{(1)})\Phi_u^{(1)}(\lambda_{\max}^{(1)})$ ^[b] [M ⁻¹ cm ⁻¹]	$10^2\Phi_u^{(1)}(\lambda_{\max}^{(1)})$ ^[b]	[BA] _∞ ^[c] [μM]	$\epsilon_u(\lambda_{\max}^{(1)}\infty)$ ^[d] [mm ⁻¹ cm ⁻¹]
NdiEt-3CN-cBA	25	443	9 ± 2	0.04 ± 0.01	15 ± 1	15 ± 1
NdiEt-3CN-cBA	4	443	3 ± 1	0.010 ± 0.002	–	11 ± 1
NdiEt-tcBA	25	472	5600 ± 600	18 ± 2	22 ± 1	23 ± 1
NdiEt-tcBA	4	472	160 ± 90	0.5 ± 0.3	–	24 ± 1
NdiEt-mcBA	25	487	11 ± 1	0.034 ± 0.004	26 ± 1	17 ± 1
NdiEt-mcBA	4	487	8 ± 1	0.024 ± 0.002	–	14 ± 1
NdiEt-cBA	5	385	51 ± 5	0.21 ± 0.02	–	17 ± 1

[a] The asymptotic normalized absorbance at the absorption maximum after uncaging, $\epsilon_u(\lambda_{\max}^{(1)}\infty)$, and concentration in benzoic acid, [BA]_∞, extracted from the fits are given in the Table. Initial concentration [cBA]₀ in caged model compound **cBA**; Solvent: acetonitrile/Tris pH 7.5 buffer (20 mM). See the main text and the Experimental Section. [b] Average obtained from the temporal dependence of the concentration in photoreleased benzoic acid measured by HPLC and the normalized absorbance. [c] Extracted from the temporal dependence of the concentration in photoreleased benzoic acid measured by HPLC. [d] Extracted from the temporal dependence of the normalized absorbance.

ure 22S, the Supporting Information). We did not observe any temporal evolution of the solution absorbance after 2 h, which suggested that **NdiEt-mcOH** was photostable. In fact, during HPLC analysis of **NdiEt-mcBA** uncaging, we observed the formation in significant amounts of a photoproduct exhibiting the same retention time and molecular weight as **NdiEt-mcOH**. In particular, the associated rate constant of $(0.020 \pm 0.001) \text{min}^{-1}$ was in fair agreement with the photo-consumption rate constant of **NdiEt-mcBA**. We thus concluded that **NdiEt-mcBA** uncaging resulted in the liberation of benzoic acid and a **NdiEt-mcOH** isomer, which we could not identify by further NMR experiments (data not shown).

The series of in vitro uncaging experiments was eventually completed by reproducing the preceding series of illumination experiments on **NdiEt-3CN-cBA**, **NdiEt-tcBA**, and **NdiEt-mcBA** at lower concentrations than 25 μM. Indeed, we were surprised by the significant discrepancy that we observed for the quantum yield of uncaging after one-photon excitation for **NdiEt-tcBA** and a thiocoumarin-caged inducer, which involved a similar leaving group (a carbamate) at the 4-coumarin benzylic position: whereas $\Phi_u^{(1)}(472)$ was about 0.2 for **NdiEt-tcBA** at 25 μM, we found $\Phi_u^{(1)}(470)$ to be about 5×10^{-3} for the thiocoumarin-caged inducer at 5 μM.^[53] Figures 18S–20S (the Supporting Information) display the temporal evolution of the absorption spectra of 4 μM solutions in 20 mM pH 7.5 Tris buffer/acetonitrile (v/v) upon illuminating at 443, 472, and 487 nm, respectively. We observed a qualitatively similar behavior to that displayed at

higher concentrations in Figures 2–4. In particular, the variation of the absorbance at the maximum of absorption could be also satisfactorily fitted with mono- (for **NdiEt-3CN-cBA** and **NdiEt-mcBA**) and bi- (for **NdiEt-tcBA**) exponential laws. After calibration of the light source, we extracted $\Phi_u^{(1)} = (1.0 \pm 0.2) \times 10^{-4}$ and $\Phi_u^{(1)} = (2.4 \pm 0.2) \times 10^{-4}$ for the quantum yield of uncaging of **NdiEt-3CN-cBA** and **NdiEt-mcBA** with one-photon excitation at $\lambda_{\max}^{(1)} = 443$ and 487 nm, respectively (see Table 3). Such values did not significantly depart from the corresponding values measured with 25 μM solutions. In contrast, we extracted $\Phi_u^{(1)} = (5 \pm 3) \times 10^{-3}$ for the quantum yield of uncaging of **NdiEt-tcBA** at $\lambda_{\max}^{(1)} = 472$ nm (see Table 3). Whereas the latter value was in excellent agreement with our result for the thiocoumarin-caged inducer illuminated at 5 μM,^[53] it was about 40 times lower than the quantum yield of uncaging of **NdiEt-tcBA** measured at 25 μM. However, we observed that the quantum yields of degradation of **NdiEt-tcOH** were essentially similar at concentrations of 4 and 25 μM (see Table 4).

Discussion

In this work, our goal was primarily to identify new coumarinylmethyl moieties exhibiting redshifted absorption together with satisfactory photochemical properties to be used as caging groups. After the present study, three caging moieties among the ten investigated can be considered as relevant for that purpose.

The **NdiEt-3CN-c** caging moiety exhibits favorable absorption, emission, and photochemical properties. It significantly absorbs at the border between UV and the visible range. It is weakly fluorescent. In addition, its uncaging quantum yield is about five times smaller than the one of the reference **NdiEt-c** coumarinylmethyl caging moiety. However, this uncaging quantum yield is notably weaker than for the recently reported DEAC450 caging group, which exhibits a similar substitution pattern to the **NdiEt-3CN-c** one.^[31] The **NdiEt-tc** caging moiety also exhibits attractive absorption, emission, and photochemical properties. It now satisfactorily absorbs in the blue-wavelength range. It is also weakly fluorescent. In the investigated range of concentration, its uncaging quantum yield is always larger than the one of the reference **NdiEt-c** coumarinylmethyl caging moiety. Nevertheless, this uncaging quantum yield significantly depends on concentration in the micromolar range. This behavior could result from the involvement of a triplet state, which is frequently observed in thiones.^[74–76] Despite our recent implementation in vivo,^[53] this feature somehow questions the robustness of the **NdiEt-tc** caging behavior in unknown media. Eventually, the **NdiEt-mc** moiety can also be considered for uncaging with cyan light; it exhibits the most redshifted absorption in our series. In contrast, as **NdiEt-c**, it is quite fluorescent, which could be a drawback

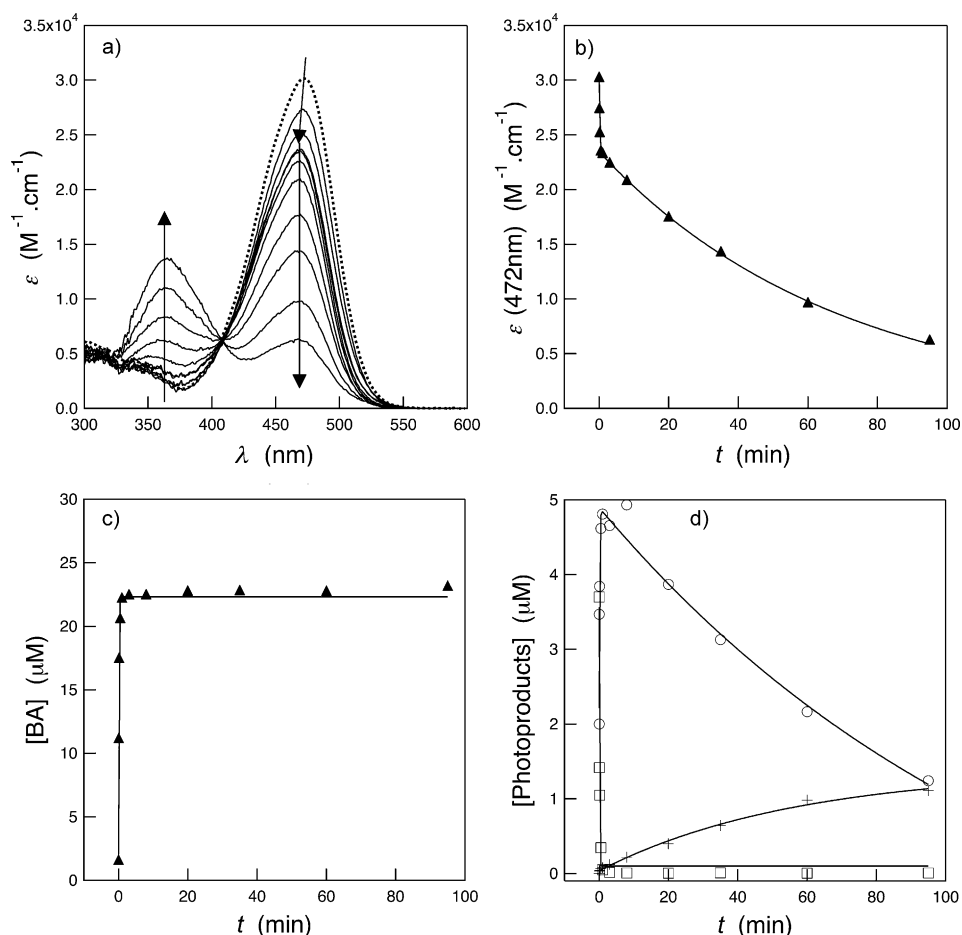


Figure 3. Evolution of a solution of **NdiEt-tcBA** ($25 \mu\text{M}$) upon illuminating at 472 nm for various durations ($I_0(472) = 6.1 \times 10^{-7} \text{ Ein min}^{-1}$; $t(\text{min}) = 0, 0.05, 0.17, 0.5, 1, 3, 8, 20, 35, 60,$ and 95). a) Temporal evolution of the solution absorbance divided by its concentration to afford its molar absorption coefficient $\varepsilon(\lambda^{(1)})$ (the initial absorption spectrum is drawn with a dotted line); b) Temporal dependence of the normalized absorption coefficient at the absorption maximum $\varepsilon(472)$ (\blacktriangle). The associated biexponential fit with Eq. (16) (see the Supporting Information) is shown as a solid line. We extracted $k_u^{(1)} = (9 \pm 1) \text{ min}^{-1}$ and $k_d^{(1)} = (0.016 \pm 0.001) \text{ min}^{-1}$, as the fastest and slowest components of the biexponential fit, respectively; c) Temporal evolution of the concentration $[\text{BA}]$ of benzoic acid extracted from the HPLC chromatogram (\blacktriangle). The exponential fit with Eq. (6) (see Supporting Information) shown as a solid line yields $k_u^{(1)} = (9 \pm 1) \text{ min}^{-1}$ and $[\text{BA}]_\infty = (22 \pm 1) \mu\text{M}$; d) Temporal evolution of the concentrations of the reactant $[\text{NdiEt-tcBA}]$ (\square) and the photoproducts $[\text{NdiEt-tcOH}]$ (\circ), and $[\text{NdiEt-cOH}]$ ($+$) extracted from the HPLC chromatogram. The global biexponential fit with Eqs. (13–15) (see the Supporting Information) shown as solid lines yields $k_u^{(1)} = (9 \pm 3) \text{ min}^{-1}$ and $k_d^{(1)} = (0.013 \pm 0.005) \text{ min}^{-1}$ as the fastest and slowest components of the biexponential fit, respectively. Solvent: $20 \text{ mM pH } 7.5$ Tris buffer/acetonitrile (v/v). $T = 293 \text{ K}$.

for several applications. Its uncaging quantum yield can be compared to the **NdiEt-3CN-c** one; it is typically ten times less efficient for uncaging than the **NdiEt-c** reference. Hence, rather large light photon fluxes should be required for uncaging. In contrast, such a low uncaging quantum yield could be advantageous to perform chromatically orthogonal photoactivations (see below).

Beyond the evaluation of the preceding caging groups in absolute terms, it is also appropriate to estimate their relevance in the context of combinations with other caging groups (or photoactive substrates) absorbing light at a different wavelength. Indeed, the orthogonal photocontrol of two different substrates with two different wavelengths has re-

cently attracted an increasing interest both for chemical and biological applications.^[41,80–86] From the latter point of view, the redshifted absorption of the **NdiEt-3CN-c**, **NdiEt-tc**, and **NdiEt-mc** caging moieties would easily permit to selectively achieve their photoactivation with respect to most classical caging groups absorbing in the UV range upon adopting a large enough excitation wavelength. Moreover, the observation that **NdiEt-3CN-c**, **NdiEt-tc**, and **NdiEt-mc** absorb light about ten times less around 365 nm than at their maximal absorption wavelength, would be also appropriate to selectively achieve the photoactivation of most UV-absorbing caging groups without significantly photoactivating **NdiEt-3CN-c**, **NdiEt-tc**, or **NdiEt-mc**. Indeed, the action uncaging cross section of the latter caging groups around 365 nm is typically two orders of magnitude smaller ($1\text{--}10 \text{ M}^{-1} \text{ cm}^{-1}$ range) than the one of most UV-absorbing caging groups, which exhibit a value of $10^2\text{--}10^3 \text{ M}^{-1} \text{ cm}^{-1}$ at that wavelength.^[6] Hence, one could easily tune either the power or the illumination duration of a 365 nm light source to selectively uncage the caging groups with maximal absorption in the UV. In fact, we already exploited the favorable features of the **NdiEt-tc** caging group in living zebrafish embryos to precisely perform chromatic orthogonal

photoactivation of two biologically active species controlling biological development with UV and blue-cyan light sources, respectively.^[53]

Conclusion

Out of ten investigated coumarinylmethyl moieties, we have identified three new caging groups that exhibit redshifted absorption together with satisfactory photochemical properties with respect to the reference 7-diethylamino coumarinylmethyl caging group. The **NdiEt-3CN-c**, **NdiEt-tc**, and **NdiEt-mc** caging moieties are synthetically easily accessible

Table 4. Action degradation cross section of the intermediate resulting from **NdiEt-tcBA** uncaging and of the alcohol **NdiEt-tcOH** for one-photon excitation at $\lambda_{\max}^{(1)}$, $\epsilon_d(\lambda_{\max}^{(1)})\Phi_d^{(1)}(\lambda_{\max}^{(1)})$ (in $\text{M}^{-1}\text{cm}^{-1}$) and quantum yield of degradation after one-photon excitation $\Phi_d^{(1)}(\lambda_{\max}^{(1)})$, as measured from the temporal dependence of the normalized absorbance and of the concentrations in reactants and photoproducts.^[a]

Compound	[tcS] [μM]	$\epsilon_d(\lambda_{\max}^{(1)})\Phi_d^{(1)}(\lambda_{\max}^{(1)})$ ^[b] [$\text{M}^{-1}\text{cm}^{-1}$]	$10^2\Phi_d^{(1)}(\lambda_{\max}^{(1)})$ ^[b]	$\Phi_d^{(1)}(\lambda_{\max}^{(1)\infty})$ ^[c] [$\text{mM}^{-1}\text{cm}^{-1}$]
NdiEt-tcBA	25	5.6 ± 1.1	0.025 ± 0.005	0 ± 1
NdiEt-tcBA	4	8 ± 1	0.036 ± 0.005	0 ± 1
NdiEt-tcOH	25	5.0 ± 0.2	0.022 ± 0.001	0 ± 1

[a] The asymptotic normalized absorbance at the absorption maximum after degradation, $\Phi_d^{(1)}(\lambda_{\max}^{(1)\infty})$, extracted from the fits is given in the Table. Initial concentration [tcS] in substrate **tcS** (**NdiEt-tcBA** or **NdiEt-tcOH**): 4 or 25 μM ; Solvent: acetonitrile/Tris pH 7.5 buffer (20 mM). See Text and Experimental Section. [b] Average from the values extracted from the temporal dependence of the concentration in photoreleased **NdiEt-tcOH** and **NdiEt-cOH** measured by HPLC, and of the normalized absorbance. [c] Extracted from the temporal dependence of the normalized absorbance.

and exhibit a significant action cross section for uncaging with blue-cyan light. Moreover their low action cross section for uncaging in the 350–400 nm wavelength range should make them attractive to perform chromatic orthogonal uncaging in combination with many presently available UV-absorbing caging groups, which do not exhibit any significant absorption beyond 450 nm. Indeed, their uncaging efficiency in this spectral domain remains significantly lower than the action cross section for uncaging of even modestly efficient UV-absorbing caging groups so as to avoid their photoactivation when a properly tuned UV illumination is applied.

Experimental Section

Reagents and solutions: Tris base (2-amino-2-(hydroxymethyl)-1,3-propanediol 99.8+ % A.C.S. reagent) and acetonitrile (spectrophotometric grade) were from Sigma–Aldrich. All solutions were prepared using water purified through a Direct-Q 5 (Millipore, Billerica, MA). All the

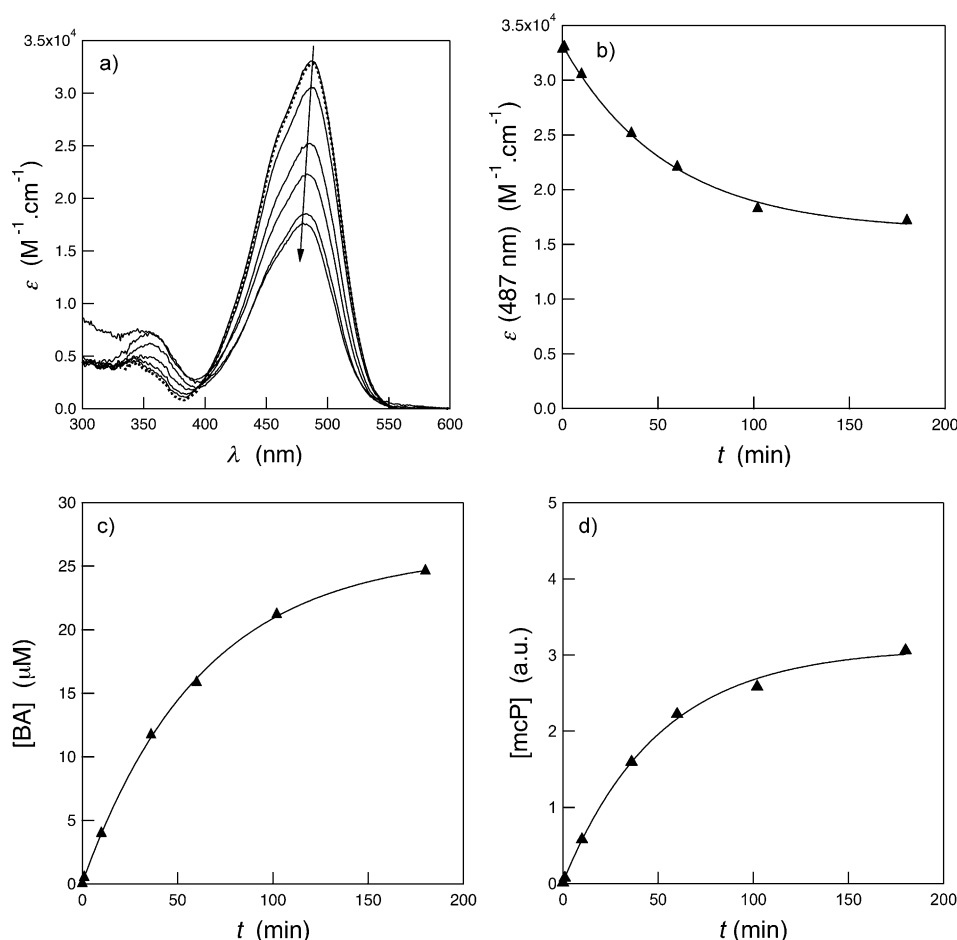


Figure 4. Evolution of a solution of **NdiEt-tcBA** (25 μM) upon illuminating at 487 nm for various durations $t(I_0(472)) = 6.1 \times 10^{-7} \text{ Ein min}^{-1}$; $t(\text{min}) = 0, 1, 10, 36, 60, 102, \text{ and } 180$. a) Temporal evolution of the solution absorbance divided by its concentration to afford its molar absorption coefficient $\epsilon(\lambda^{(1)})$ (the initial absorption spectrum is drawn with a dotted line); b) Temporal dependence of the normalized absorbance coefficient at the absorption maximum $\epsilon(487)$ (\blacktriangle). The associated exponential fit with Eq. (9) (see the Supporting Information) is shown as a solid line. We extracted $k_u^{(1)} = (0.018 \pm 0.001) \text{ min}^{-1}$ from the exponential fit; c) Temporal evolution of the concentration [BA] of benzoic acid extracted from the HPLC chromatogram (\blacktriangle). The exponential fit with Eq. (6) (see the Supporting Information) shown as a solid line yields $k_u^{(1)} = (0.016 \pm 0.002) \text{ min}^{-1}$ and $[\text{BA}]_{\infty} = (26 \pm 1) \mu\text{M}$; d) Temporal evolution of the concentration [mcP] of the photoproduct extracted from the HPLC chromatogram (\blacktriangle). The exponential fit with Eq. (6) (see the Supporting Information) shown as a solid line yields $k_u^{(1)} = (0.02 \pm 0.01) \text{ min}^{-1}$. Solvent: 20 mM pH 7.5 Tris buffer/acetonitrile (v/v). $T = 293 \text{ K}$.

experiments were performed at 293 K in a buffered solution obtained by mixing in equal volumes acetonitrile and a 20 mM Tris base aqueous solution acidified to 7.5 (evaluated from glass electrode reading with a pH-meter PHM 210; Radiometer Analytical calibrated at pH 4 and 7) with 1 M chlorhydric acid.

Photophysical properties: The UV/Vis absorption spectra were recorded on a Kontron Uvikon-940 spectrophotometer at 293 K. Molar absorption coefficients were extracted while checking the validity of the Beer–Lambert law.

Corrected emission spectra upon one-photon excitation were obtained from a Photon Technology International QuantaMaster spectrofluorimeter. Solutions for emission measurements were adjusted to concentrations such that the absorption maximum was around 0.15 at the excitation wavelength. The overall emission quantum yields after one-photon excitation $\Phi_{\text{em}}^{(1)}$ values were calculated from the following relation:

$$\Phi_{\text{em}}^{(1)} = \Phi_{\text{ref}}^{(1)} \frac{1 - 10^{-A_{\text{ref}}(\lambda_{\text{exc}})}}{1 - 10^{-A(\lambda_{\text{exc}})}} \frac{D}{D_{\text{ref}}} \left(\frac{n}{n_{\text{ref}}} \right)^2$$

in which the subscript “ref” stands for standard samples, $A_{\text{ref}}(\lambda_{\text{exc}})$ is the absorbance at the excitation wavelength, D is the integrated emission spectrum, and n is the refractive index for the solvent. The uncertainty in the experimental value of $\Phi_{\text{em}}^{(1)}$ was estimated to be $\pm 10\%$. The standard fluorophore for the quantum yields measurements was fluorescein in sodium hydroxide (0.1 M) with $\Phi_{\text{ref}}^{(1)} = 0.92$.^[87]

The quartz cuvettes (Hellma) were either 1 × 1 cm (3 mL samples) or 1 × 0.2 cm (0.4 mL samples). The holders were thermostated using circulating baths (Polystat 34-R2, Fisher Bioblock Scientific, Illkirch, France) and the temperature was directly measured in the cuvettes by using a type K thermocouple connected to a ST-610B digital pyrometer (Stafford Instruments, Stafford, UK).

HPLC coupled to mass spectrometry: High-pressure liquid chromatography was carried out by using an Accela System liquid chromatograph (Thermo Finnigan, Les Ulis, France) equipped with a Hypersil Gold column (1.9 $\mu\text{m} \times 2.1 \times 50$ mm) connected to a Thermo-Finnigan TSO Quantum Discovery Max triple quadrupole mass spectrometer. The illuminated sample solution (5 μL) was injected in the chromatographic column. The analyte eluted from the column with a mobile phase composed of two solvents A (water containing formic acid at 0.05% v/v) and B (acetonitrile). A gradient was used to optimize the separation of the analytes. Initially, the column was equilibrated at 200 $\mu\text{L min}^{-1}$ with a mobile phase consisting of 90% A and 10% B. One minute after the injection, the proportion of B was linearly increased to 85% within 4 min and at that position for two additional minutes. After this step, composition of the mobile phase was set to initial and the column was equilibrated for 3 min prior to next injection. After separation, the analytes (except benzoic acid) were introduced in the mass spectrometer through a heated electrospray ionization source (50 °C, 4000 V) operating in the positive mode. The temperature of the capillary transfer was set at 270 °C. Nitrogen was employed as nebulizing (35 psi) and auxiliary gas (30 arbitrary units). Argon was used as collision gas (1.0 milliTorr in Q2). Again peak areas were converted into concentrations after preliminary calibrations. Instrument control and data collection were handled by a computer equipped with Xcalibur software (version 2.0).

In the case of benzoic acid, the HPLC system consisted of a Dionex HPLC P680A LPG-4 pump, a Dionex ASI-100 autosampler, and a Dionex UVD 340U UV detector or an Agilent 1260 Chromatographic system. Instrument control and data collection were handled by a computer equipped with Chromeleon software. Samples (10 or 20 μL) were injected on Kinetex C₁₈ columns (50 × 2.1 mm or 4.6 × 100 mm, 2.6 μm , Phenomenex, Torrance, CA), and benzoic acid eluted out of the column in isocratic mode with a mixture of water containing 0.1% formic acid and acetonitrile (65–35 v/v) at a flow rate of 0.5 or 1 mL min⁻¹. Benzoic acid was detected by UV absorption at 227 nm and the conversion of the peak area to the solution concentration was achieved from a preliminary calibration.

Irradiation experiments with one-photon excitation: Two different protocols have been used to perform the irradiations relying on one-photon excitation.

Preliminary illuminations at 365 nm: One-photon illumination experiments were performed at 20 °C, with a benchtop UV lamp^[88] (365 nm, essentially a 40 nm-wide, at half height, Gaussian distribution centered at 350 nm; Fisher Bioblock) delivering typical 1.0×10^{-2} Einstein min⁻¹ m⁻² surfacic photon fluxes (measured using the reference PheP reported in reference [88]) in the illuminated 25 μm sample (20 mL) contained in a cylindrical glass dish: diameter 8.5 cm; height: 2.0 cm. Aliquots (3 mL) were withdrawn after given durations of illumination for recording a UV/Vis absorption spectrum and put back into the glass dish for further irradiation. Aliquots (200 μL) were independently extracted after various illumination times and kept at -18 °C for HPLC analysis.

Illumination at the absorption maxima: The illumination experiments performed at the maximum of absorption of the caged substrates selected after the preliminary screening at 365 nm were performed with the 75 W xenon lamp of the spectrofluorometer. We also notably used this configuration with 365 nm excitation to perform control experiments.

We made two series of illumination experiments associated to different concentrations of caged substrate:

Concentrated solutions (typically 25 μM as 0.4 mL samples in 1 × 0.2 cm² quartz cuvettes under constant stirring; 1 cm illumination pathway) were used to facilitate the HPLC analysis leading to identify and quantify the photoproducts. One sample (0.4 mL) was used for each illumination delay. After illumination, a sample (200 μL) was removed and kept at -18 °C before performing the concentration-demanding analysis of benzoic acid by HPLC with UV detection. The remaining mother solution was diluted by a factor five and the resulting daughter solution was subsequently used for analysis with HPLC/Mass spectrometry and UV/Vis absorption;

More diluted solutions (typically 5 μM as 3 mL samples in 1 × 1 cm² quartz cuvettes under constant stirring; absorbance at the excitation wavelength lower than 0.15) were used to monitor the absorbance of the sample during illumination.

Light intensity at the excitation wavelength $\Phi_{\text{exc}}^{(1)}$ was systematically calibrated before each experiment using a procedure relying on analyzing the intensity I_{DCM} of fluorescence emission of a 4-dicyanomethylene-2-methyl-6-*p*-dimethylamino-styryl-4H-pyrene (DCM) solution in absolute ethanol upon exciting at two different wavelengths. The fluorescence emission $I_{\text{DCM}}(\Phi_{\text{exc}}^{(1)})$ associated to $I_0(\Phi_{\text{exc}}^{(1)})$ was first recorded upon exciting at $\Phi_{\text{exc}}^{(1)}$, in which DCM absorbs light with a molar absorption coefficient $\epsilon_{\text{DCM}}(\Phi_{\text{exc}}^{(1)})$. Then, the corresponding fluorescence emission $I_{\text{DCM}}(365)$ was recorded upon exciting at 365 nm with light intensity $I_0(365)$ (molar absorption coefficient $\epsilon_{\text{DCM}}(365)$). $I_0(365)$ was subsequently extracted from determining the kinetics of photoconversion at 365 nm of the α -(4-dimethylaminophenyl)-*N*-phenylnitron into 3-(4-dimethylaminophenyl)-2-phenyloxaziridine in absolute ethanol as described in reference [89]. Eventually, the light intensity $I_0(\Phi_{\text{exc}}^{(1)})$ was computed from $\frac{\epsilon_{\text{DCM}}(365)/\epsilon_{\text{DCM}}(\lambda_{\text{exc}}^{(1)})}{\epsilon_{\text{DCM}}(\lambda_{\text{exc}}^{(1)})/I_{\text{DCM}}(365)} I_0(365)$. During the present series of experiments, typical overall photon fluxes at the sample were in the 10^{-6} – 10^{-7} Eins⁻¹ range.

Acknowledgements

This work has been supported by the ANR (PCV 2008, Proteophane) and the Ministère de la Recherche (for a fellowship to L.F.). The authors thank Dr. V. Jullien and Prof. G. Pons at Service de Pharmacologie Clinique, Saint Vincent de Paul Hospital Paris, for access to their HPLC-MS instrument. The authors declare no competing financial interests.

- [1] V. N. Rajasekharan Pillai, *Synthesis* **1980**, 1–26.
- [2] C. G. Bochet, *J. Chem. Soc. Perkin Trans. 1* **2002**, 125–142.
- [3] A. P. Pelliccioli, J. Wirz, *Photochem. Photobiol. Sci.* **2002**, *1*, 441–458.

- [4] *Dynamic Studies in Biology* (Eds.: M. Goeldner, R. Givens), Wiley-VCH, Weinheim, **2005**.
- [5] G. Mayer, A. Heckel, *Angew. Chem.* **2006**, *118*, 5020–5042; *Angew. Chem. Int. Ed.* **2006**, *45*, 4900–4921.
- [6] G. C. R. Ellis-Davies, *Nat. Methods* **2007**, *4*, 619–628.
- [7] D. D. Young, A. Deiters, *Org. Biomol. Chem.* **2007**, *5*, 999–1005.
- [8] H.-M. Lee, D. R. Larson, D. S. Lawrence, *ACS Chem. Biol.* **2009**, *4*, 409–427.
- [9] A. Specht, F. Bolze, Z. Omran, J.-F. Nicoud, M. Goeldner, *HFSP J.* **2009**, *3*, 255–264.
- [10] H. Yu, J. Li, D. Wu, Z. Qiu, Y. Zhang, *Chem. Soc. Rev.* **2010**, *39*, 464–473.
- [11] A. Deiters, *ChemBioChem* **2009**, *11*, 47–53.
- [12] C. Bricke, F. Rohrbach, A. Gottschalk, G. Mayer, A. Heckel, *Angew. Chem. Int. Ed.* **2012**, *51*, 8446–8476.
- [13] P. Klán, T. Solomek, C. G. Bochet, A. Blanc, R. Givens, M. Rubina, V. Popik, A. Kostikov, J. Wirz, *Chem. Rev.* **2013**, *113*, 119–191.
- [14] J. Baier, T. Maisch, M. Maier, E. Engel, M. Landthaler, W. Baumler, *Biophys. J.* **2006**, *91*, 1452–1459.
- [15] G. Kick, G. Messer, G. Plewig, P. Kind, A. E. Goetz, *Br. J. Cancer* **1996**, *74*, 30–36.
- [16] L.-O. Klotz, C. Pellioux, K. Briviba, C. Pierlot, J.-M. Aubry, H. Sies, *Eur. J. Biochem.* **1999**, *260*, 917–922.
- [17] K. Wertz, N. Seifert, P. Buchwald Hunziker, G. Riss, A. Wyss, W. Hunziker, R. Goralczyk, *Pure Appl. Chem.* **2006**, *78*, 1539–1550.
- [18] Y. Chen, M. G. Steinmetz, *Org. Lett.* **2005**, *7*, 3729–3732.
- [19] Y. Chen, M. G. Steinmetz, *J. Org. Chem.* **2006**, *71*, 6053–6060.
- [20] P. Sebej, J. Wintner, P. Müller, T. Slanina, J. A. Anshori, L. A. P. Antony, P. Klan, J. Wirz, *J. Org. Chem.* **2013**, *78*, 1833–1843.
- [21] L. Zayat, C. Calero, P. Albores, L. Baraldo, R. Etchenique, *J. Am. Chem. Soc.* **2003**, *125*, 882–883.
- [22] L. Zayat, M. Salierno, R. Etchenique, *Inorg. Chem.* **2006**, *45*, 1728–1731.
- [23] L. Zayat, M. G. Noval, J. Campi, C. I. Calero, D. J. Calvo, R. Etchenique, *ChemBioChem* **2007**, *8*, 2035–2038.
- [24] M. Salierno, C. Fameli, R. Etchenique, *Eur. J. Inorg. Chem.* **2008**, 1125–1128.
- [25] E. M. Rial Verde, L. Zayat, R. Etchenique, R. Yuste, *Front. Neural Circuits* **2008**, *2*, 1–7.
- [26] K. Lee, D. E. Falvey, *J. Am. Chem. Soc.* **2000**, *122*, 9361–9366.
- [27] C. Sundararajan, D. E. Falvey, *J. Am. Chem. Soc.* **2005**, *127*, 8000–8001.
- [28] J. B. Borak, S. López-Sola, D. E. Falvey, *Org. Lett.* **2008**, *10*, 457–460.
- [29] S. Gug, F. Bolze, A. Specht, C. Bourgoigne, M. Goeldner, J.-F. Nicoud, *Angew. Chem.* **2008**, *120*, 9667–9671; *Angew. Chem. Int. Ed.* **2008**, *47*, 9525–9529.
- [30] L. Donato, A. Mourot, C. M. Davenport, C. Herbivo, D. Warther, J. Léonard, F. Bolze, J.-F. Nicoud, R. H. Kramer, M. Goeldner, A. Specht, *Angew. Chem. Int. Ed.* **2012**, *51*, 1840–1843.
- [31] J. P. Olson, H.-B. Kwon, K. T. Takasaki, Q. Chiayu, C. Q. Chiu, M. J. Higley, B. L. Sabatini, G. C. R. Ellis-Davies, *J. Am. Chem. Soc.* **2013**, *135*, 5954–5957.
- [32] I. Aujard, C. Benbrahim, M. Gouget, O. Ruel, J. B. Baudin, P. Neveu, L. Jullien, *Chem. Eur. J.* **2006**, *12*, 6865–6879.
- [33] R. S. Givens, B. Matuszewski, *J. Am. Chem. Soc.* **1984**, *106*, 6860–6861.
- [34] T. Furuta, H. Torigai, T. Osawa, M. Iwamura, *J. Org. Chem.* **1995**, *60*, 3953–3956.
- [35] T. Furuta, M. Iwamura, *Methods Enzymol.* **1998**, *291*, 50–63.
- [36] R. S. Givens, M. Rubina, J. Wirz, *Photochem. Photobiol. Sci.* **2012**, *11*, 472–488.
- [37] T. Furuta, S. S.-H. Wang, J. L. Dantzker, T. M. Dore, W. J. Bybee, E. M. Callaway, W. Denk, R. Y. Tsien, *Proc. Natl. Acad. Sci. USA* **1999**, *96*, 1193–1200.
- [38] R. O. Schönleber, J. Bendig, V. Hagen, B. Giese, *Bioorg. Med. Chem.* **2002**, *10*, 97–101.
- [39] W. Lin, D. S. Lawrence, *J. Org. Chem.* **2002**, *67*, 2723–2726.
- [40] A. Z. Suzuki, T. Watanabe, M. Kawamoto, K. Nishiyama, H. Yamashita, M. Ishii, M. Iwamura, T. Furuta, *Org. Lett.* **2003**, *5*, 4867–4870.
- [41] N. Kotzur, B. Briand, M. Beyermann, V. Hagen, *J. Am. Chem. Soc.* **2009**, *131*, 16927–16931.
- [42] V. Hagen, F. Kilic, J. Schaal, B. Dekowski, R. Schmidt, N. Kotzur, *J. Org. Chem.* **2010**, *75*, 2790–2792.
- [43] V. Hagen, J. Bendig, S. Frings, B. Wiesner, B. Schade, S. Helm, D. Lorenz, U. B. Kaupp, *J. Photochem. Photobiol. B* **1999**, *53*, 91–102.
- [44] M. Skwarczynski, M. Noguchi, S. Hirota, Y. Sohma, T. Kimura, Y. Hayashi, Y. Kiso, *Bioorg. Med. Chem. Lett.* **2006**, *16*, 4492–4496.
- [45] T. Eckardt, V. Hagen, B. Schade, R. Schmidt, C. Schweitzer, J. Bendig, *J. Org. Chem.* **2002**, *67*, 703–710.
- [46] B. Schade, V. Hagen, R. Schmidt, R. Herbrich, E. Krause, T. Eckardt, J. Bendig, *J. Org. Chem.* **2002**, *67*, 703–710.
- [47] R. Schmidt, D. Geissler, V. Hagen, J. Bendig, *J. Phys. Chem. A* **2005**, *109*, 5000–5004.
- [48] V. Hagen, S. Frings, B. Wiesner, S. Helm, U. B. Kaupp, J. Bendig, *ChemBioChem* **2003**, *4*, 434–442.
- [49] T. Furuta, H. Takeuchi, M. Isozaki, Y. Takahashi, M. Kanehara, M. Sugimoto, T. Watanabe, K. Noguchi, T. M. Dore, T. Kurahashi, M. Iwamura, R. Y. Tsien, *ChemBioChem* **2004**, *5*, 1119–1128.
- [50] V. R. Shembekar, Y. Chen, B. K. Carpenter, G. P. Hess, *Biochemistry* **2005**, *44*, 7107–7114.
- [51] C. Bao, G. Fan, Q. Lin, B. Li, S. Cheng, Q. Huang, L. Zhu, *Org. Lett.* **2012**, *14*, 572–575.
- [52] A. S. C. Fonseca, A. M. S. Soares, M. S. T. Goncalves, S. P. G. Costa, *Tetrahedron* **2012**, *68*, 7892–7900.
- [53] L. Fournier, C. Gauron, L. Xu, I. Aujard, T. Le Saux, N. Gagey-Eilstein, S. Maurin, S. Dubruille, J.-B. Baudin, D. Bensimon, M. Volovitch, S. Vríz, L. Jullien, *ACS Chem. Biol.*, **2013**, *8*, 1528–1536.
- [54] M. A. Kirpichénok, V. M. Baukulev, L. A. Karandashova, *Chem. Heterocycl. Compd.* **1991**, *27*, 1193–1199.
- [55] I. I. Tkach, A. V. Reznichenko, E. A. Lukyanets, *Chem. Heterocycl. Compd.* **1992**, *28*, 872–880.
- [56] J. Yu, Y. Shirota, *Chem. Lett.* **2002**, *31*, 984–985.
- [57] K. Komatsu, Y. Urano, H. Kojima, T. Nagano, *J. Am. Chem. Soc.* **2007**, *129*, 13447–13454.
- [58] M. Wilcox, R. W. Viola, K. W. Johnson, A. P. Billington, B. K. Carpenter, J. A. McCray, A. P. Guzikowski, G. P. Hess, *J. Org. Chem.* **1990**, *55*, 1585–1589.
- [59] B. Schade, V. Hagen, R. Schmidt, R. Herbrich, J. Bendig, *J. Org. Chem.* **1999**, *64*, 9109–9117.
- [60] A. M. Piloto, A. S. C. Fonseca, S. P. G. Costa, M. S. T. Gonçalves, *Tetrahedron* **2006**, *62*, 9258–9276.
- [61] S. Scheibye, J. Kristensen, S.-O. Lawesson, *Tetrahedron* **1979**, *35*, 1339–1343.
- [62] J. N. Gadre, A. A. Audi, N. P. Karambelkar, *Ind. J. Chem.* **1996**, *35B*, 60–62.
- [63] M. Yokoyama, M. Irie, K. Sujino, T. Kagemoto, H. Togo, M. Funabashi, *J. Chem. Soc. Perkin Trans. 1* **1992**, 2127–2134.
- [64] W. Przychodzeń, *Eur. J. Org. Chem.* **2005**, 2002–2014. W. Przychodzeń, *J. Chem. Soc. Perkin Trans. 1* **1992**, 2127–2134.
- [65] P. N. Bhargava, S. Prakash, *J. Indian Chem. Soc.* **1979**, *56*, 937–938.
- [66] P. Reynaud, J.-D. Brion, G. Ménard, *Bull. Soc. Chim. Fr.* **1976**, *1*–2, 301–306.
- [67] Ya. L. Garazd, M. M. Garazd, V. A. Turov, V. P. Khilya, *Chem. Nat. Compd.* **2006**, *42*, 652–655.
- [68] P. Stegmaier, J. M. Alonso, A. del Campo, *Langmuir* **2008**, *24*, 11872–11879.
- [69] K. Ito, J. Maruyama, *Chem. Pharm. Bull.* **1983**, *31*, 3014–3023.
- [70] H. Abdel-Ghany, H. M. Moustafa, A. Khodairy, *Synth. Commun.* **1998**, *28*, 3431–3441.
- [71] N. Latif, I. Fathy, *Can. J. Chem.* **1966**, *44*, 1075–1081.
- [72] S. S. Lele, M. G. Patel, S. Sethna, *J. Org. Chem.* **1962**, *27*, 637–639.
- [73] K. H. Al-Zghoul, K. S. M. Salih, M. T. Ayoub, M. S. Mubarak, *Heterocycles* **2005**, *65*, 2937–2947.
- [74] R. P. Steer, V. Ramamurthy, *Acc. Chem. Res.* **1988**, *21*, 380–386.
- [75] A. Maciejewski, R. P. Steer, *Chem. Rev.* **1993**, *93*, 67–98.

- [76] a) K. Bhattacharyya, P. K. Das, V. Ramamurthy, V. P. Rao, *J. Chem. Soc. Faraday Trans. 2* **1986**, *82*, 135–147; b) S. Devanathan, V. Ramamurthy, *J. Org. Chem.* **1988**, *53*, 741–744; c) R. S. Becker, S. Chakravorty, C. A. Gartner, M. de Graca Miguel, *J. Chem. Soc. Faraday Trans.* **1993**, *89*, 1007–1019; d) G. Burdzinska, G. Buntinx, O. Poizat, C. Lapouge, *J. Mol. Struct.* **2005**, *735–736*, 115–122.
- [77] We cannot exclude that thermal stability could be substrate dependent. Hence, Ellis–Davies caged glutamate with the **NdiEt-tc** caging moiety to yield **NdiEt-tc-Glu** (personal communication). In contrast to our observations with **NdiEt-tc-BA**, as well as with a **NdiEt-tc**-caged inducer reported in Reference [53], he observed that **NdiEt-tc-Glu** was rapidly converted in 1 h to **NdiEt-c-Glu** in methanol (MeOD) or 1% methanol in HEPES pH 7.4.
- [78] In fact, we observed that UV illumination caused a slow increase of absorbance. However, the corresponding photochemical reaction did not lead to the release of benzoic acid.
- [79] In the absence of any illumination, we checked that the **NdiEt-tcOH** solution was thermally stable at the timescale of the illumination experiment (typically, 3 h).
- [80] C. G. Bochet, *Angew. Chem.* **2001**, *113*, 2140–2142; *Angew. Chem. Int. Ed.* **2001**, *40*, 2071–2073.
- [81] S. Kantevari, M. Matsuzaki, Y. Kanemoto, H. Kasai, G. C. R. Ellis-Davies, *Nat. Methods* **2010**, *7*, 123–125.
- [82] D. Goguen, A. Aemissegger, B. Imperiali, *J. Am. Chem. Soc.* **2011**, *133*, 11038–11041.
- [83] M. Priestman, L. Sun, D. S. Lawrence, *ACS Chem. Biol.* **2011**, *6*, 377–384.
- [84] V. San Miguel, C. G. Bochet, A. del Campo, *J. Am. Chem. Soc.* **2011**, *133*, 5380–5388.
- [85] C. Menge, A. Heckel, *Org. Lett.* **2011**, *13*, 4620–4623.
- [86] M. N. Stanton-Humphreys, R. D. T. Taylor, C. McDougall, M. L. Hart, C. Tom, A. Brown, N. J. Emptage, S. J. Conway, *Chem. Commun.* **2012**, *48*, 657–659.
- [87] J. N. Demás, G. A. Crosby, *J. Phys. Chem.* **1971**, *75*, 991–1024.
- [88] a) P. Neveu, I. Aujard, C. Benbrahim, T. Le Saux, J.-F. Allemand, S. Vríz, D. Bensimon, L. Jullien, *Angew. Chem.* **2008**, *120*, 3804–3806; *Angew. Chem. Int. Ed.* **2008**, *47*, 3744–3746; b) P. Neveu, D. Sinha, P. Kettunen, S. Vríz, L. Jullien, D. Bensimon in *Nobel Volume on Single Molecule Spectroscopy in Chemistry, Physics and Biology*, Springer, Heidelberg, **2009**; c) D. K. Sinha, P. Neveu, N. Gagey, I. Aujard, C. Benbrahim-Bouzidi, T. Le Saux, C. Rampon, C. Gauron, B. Goetz, S. Dubrulle, M. Baaden, M. Volovitch, D. Bensimon, S. Vríz, L. Jullien, *ChemBioChem* **2010**, *11*, 653–663; d) D. K. Sinha, P. Neveu, N. Gagey, I. Aujard, T. Le Saux, C. Rampon, C. Gauron, K. Kawakami, C. Leucht, L. Bally-Cuif, M. Volovitch, D. Bensimon, L. Jullien, S. Vríz, *Zebrafish* **2010**, *7*, 199–204.
- [89] P. F. Wang, L. Jullien, B. Valeur, J.-S. Filhol, J. Canceill, J.-M. Lehn, *New J. Chem.* **1996**, *20*, 895–907.

Received: July 6, 2013

Revised: August 16, 2013

Published online: November 11, 2013